Proc. Natl. Acad. Sci. USA
Vol. 83, pp. 8972–8976, December 1986
Biophysics

Stoichiometric model of the photosynthetic unit of *Ectothiorhodospira halochloris*

(mass mapping/scanning transmission electron microscopy/image processing/three-dimensional reconstruction/bacterial photosynthetic membrane)

HARALD ENGELHARDT*, ANDREAS ENGEL†, AND WOLFGANG BAUMEISTER*

*Max-Planck-Institut für Biochemie, D-8033 Martinsried, Federal Republic of Germany; and †Microbiology Department, Biozentrum, University of Basel, Klingelbergstrasse 70, CH-4056 Basel, Switzerland

Communicated by Albert V. Crewe, August 1, 1986

ABSTRACT **A stoichiometric model of the photosynthetic unit of *Ectothiorhodospira halochloris* has been obtained by means of scanning transmission electron microscope mass determination and mass mapping in conjunction with polyacrylamide gel electrophoresis. One reaction center, consisting of four single polypeptides, including one cytochrome, is surrounded by six identical light-harvesting complexes, each containing three polypeptides with 2:2:2 stoichiometry. This stoichiometric model was incorporated into the three-dimensional structure of the photosynthetic unit as derived from surface relief reconstructions of the two surfaces of shadowed membranes. The reaction center protrudes substantially from both membrane surfaces and has the cytochrome attached to the periplasmic face in a noncentrosymmetric fashion. The reaction center may assume various orientations within the photosynthetic complexes.**

The photosynthetic membranes of bacteriochlorophyll b-containing bacteria, particularly of *Rhodopseudomonas viridis* and *Ectothiorhodospira halochloris*, have previously been studied by electron microscopy and image processing, and several models of the photosynthetic unit have been proposed (1–5). They agree as far as the hexagonal arrangement of the complexes in the membranes with lattice spacings of approximately 13 nm is concerned, and in the gross morphology of the photosynthetic units, which consist of a central core, the reaction center (RC), surrounded by a ring of light-harvesting (LH) complexes. The models differ, however, with respect to the number and arrangement of LH subunits.

In this study we present a low-resolution stoichiometric model of the photosynthetic unit from *E. halochloris*. We have applied scanning transmission electron microscope (STEM) mass determination (6) and mass mapping (7). These methods are capable of determining the masses of small discrete features within a large protein complex; it is in fact the only way of measuring masses of membrane constituents *in situ* without disintegrating the structures of interest. Mass mapping, in conjunction with polyacrylamide gel electrophoresis (PAGE) of the photosynthetic membranes, enabled us to determine the stoichiometric polypeptide composition in the photosynthetic unit. The three-dimensional structure of the photosynthetic complex was obtained by surface relief reconstruction (8) from unidirectionally shadowed membranes.

MATERIALS AND METHODS

Membrane Preparation. Cells of *E. halochloris* (DSM 1059) were grown anaerobically in the light as described previously (9). Membranes were either rapidly prepared by spheroplast formation (5) for electron microscopy or purified for PAGE as follows. Washed cells were resuspended in a 0.3 M Tris/tartrate buffer solution, pH 7.0, and disintegrated in a French press at 70 MPa (10,000 pounds/inch^2) and approximately 5°C. Membranes, collected by differential centrifugation, were washed repeatedly and centrifuged for 15 hr on a 10–60% metrizamide (Nyegaard, Oslo) density gradient at 140,000 × g. The dark green band was purified from metrizamide and used for PAGE.

PAGE. The membranes (50 μg of protein) were resuspended in sample buffer solution consisting of 50 mM sodium carbonate, 50 mM dithioerythritol, 10% sucrose, and 2% $LiDodSO_4$ (final concentrations) and incubated 15 min at 30°C. The gel system according to ref. 10 was used, omitting urea and $NaDodSO_4$. The gels were 25 cm long, 17.5 cm wide, and 1.5 mm thick, and electrophoresis was for 15 hr at 5°C with a constant current of 20 mA. Protein was stained with Coomassie brilliant blue R250; heme (peroxidase activity) staining and destaining was performed according to ref. 11. Polypeptides in the molecular mass range of 3–12 kDa were calibrated with myoglobin fragments (Pharmacia), insulin A and B chains, and aprotinin. Gels stained for heme-containing proteins were calibrated with cytochrome *c* cross-linked as follows. Cytochrome *c* from rabbit muscle (50 mg) was dissolved in 1 ml of 50 mM triethanolamine buffer solution at pH 9.0, dimethylsuberimidate dissolved in dimethyl sulfoxide was added in three portions every 10 min to a final concentration of 10 mM, the mixture was incubated at 35°C, and the reaction was stopped after 30 min by 67 mM (final concentration) Tris·HCl, pH 8.0. Cross-linked cytochrome *c* was applied to the gels in 20-μg portions.

Electron Microscopy. Freshly prepared membranes derived from spheroplasts (5) were either negatively stained with 1.5% sodium phosphotungstate, pH 6.8, or quickly frozen in liquid nitrogen. Subsequent freeze-drying was performed either in a Balzers 500K freeze-etching machine for shadowing purposes (tungsten/tantalum) (5), or according to ref. 7 for mass determination with the STEM. Negatively stained and shadowed membranes were recorded at 80 kV in a Philips 420 electron microscope at magnifications of ×36,000 or ×60,000. Appropriate areas of the electron micrographs were digitized (1024 pixels square) at 0.37- or 0.46-nm intervals at the specimen level. Elastic dark-field images (512 points square) were recorded in a Vacuum Generators HB5 STEM at 80 kV and stored on magnetic tape. The scanning interval was 0.91 nm. Images were recorded with doses between 300 and 1000 electrons per nm^2; a maximum mass loss of 5–10% has to be accounted for in this dose range (6, 7).

The publication costs of this article were defrayed in part by page charge payment. This article must therefore be hereby marked "*advertisement*" in accordance with 18 U.S.C. §1734 solely to indicate this fact.

Abbreviations: RC, reaction center; LH, light-harvesting; STEM, scanning transmission electron microscope; PAGE, polyacrylamide gel electrophoresis.

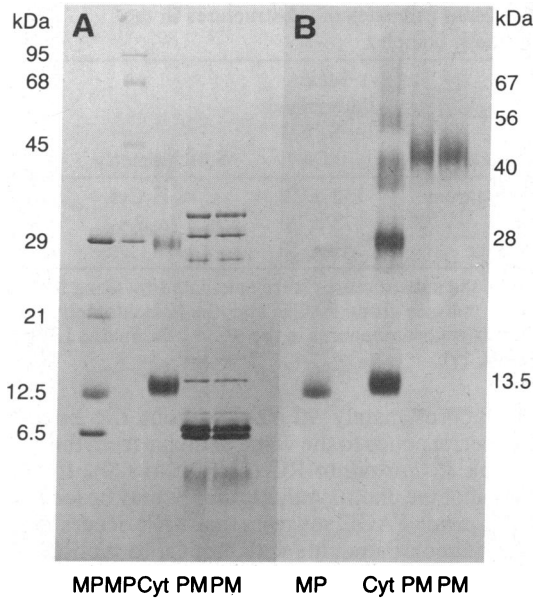

FIG. 1. LiDodSO$_4$/PAGE of photosynthetic membranes from *E. halochloris*. (*A*) Coomassie blue-stained protein bands. (*B*) Heme (peroxidase activity) staining of cytochromes. MP, marker proteins with molecular masses given; Cyt, cross-linked cytochrome *c*; PM, photosynthetic membrane proteins.

Image Processing. The images were averaged by correlation methods according to ref. 12. Averages of positions with high correlation coefficients were refined by applying strain selection (13). Correspondence analysis (14) and surface relief reconstruction (8) of heavy-metal-shadowed membranes were performed as described in detail previously (5). For STEM dark-field images of unstained membranes with very low signal-to-noise ratios, references were obtained by quasi-optical filtration, extracting areas usually 4 times the lattice spacing in size.

STEM Mass Determination and Mass Mapping. These procedures were performed as described in detail previously (6, 7). The boundaries of the substructures to be analyzed were defined by means of averages from negatively stained membranes and surface relief reconstructions. The photosynthetic complexes were masked off outside the selected areas, and the grey levels were evaluated, integrated over the particular areas, and finally calibrated relative to the total mass of the unit cell.

Table 1. Apparent molecular masses of polypeptides from the photosynthetic membranes

Polypeptide band in LiDodSO4 gels	Apparent molecular mass, kDa
Cytochrome	41 ± 2
H	33 ± 2
M	30 ± 2
L	27 ± 2
"X"	15 ± 1
α	7.8 ± 0.7
β	6.0 ± 0.2
γ	3.7 ± 0.8

The figures are mean ± SD values from seven gels.

RESULTS AND DISCUSSION

The photosynthetic membranes have a characteristic polypeptide pattern in LiDodSO$_4$ gels (Fig. 1). Four bands with apparent molecular masses of 27, 30, 33, and 41 kDa occur in the RC region (Table 1); the largest polypeptide, which smeared in LiDodSO$_4$ gels, was identified as a cytochrome. A few minor heme-containing bands were found with apparent molecular masses of 32, 22, and 9 kDa, but they were very weakly stained, suggesting that these cytochromes are not components of the photosynthetic complexes. The 27- and 30-kDa polypeptides (Table 1) tend to aggregate upon incubation above 30°C, creating a new band at about 60 kDa; this behavior is typical of the L and M subunits from bacterial RCs (15). The 15-kDa protein remains to be identified, but it is likely to be a component of the photosynthetic unit (16). The ratios of the integrated staining intensities (not corrected for individual dye binding) for the bands "X," L, M, H, and cytochrome are 0.7:0.8:0.94:1:0.9.

The LH polypeptide region contains two identically stained bands (α and β), accompanied by a third, weakly stained, polypeptide (γ, Table 1). The latter can be solubilized by extraction with methanol/chloroform, indicating a very hydrophobic character. Previously this small protein had been observed only in membranes of *R. viridis*; despite its different staining it is thought to occur in equimolar amounts with respect to the α and β polypeptides (17). The apparent molecular masses of the LH polypeptides are in good agreement with the sequence data of the corresponding proteins from *R. viridis* (4.00, 6.14, and 6.85 kDa) (17).

The total mass of the photosynthetic unit, including chromophores and lipids, was determined *in situ* with freshly prepared and freeze-dried membranes by means of STEM. The images were recorded under moderate low-dose condi-

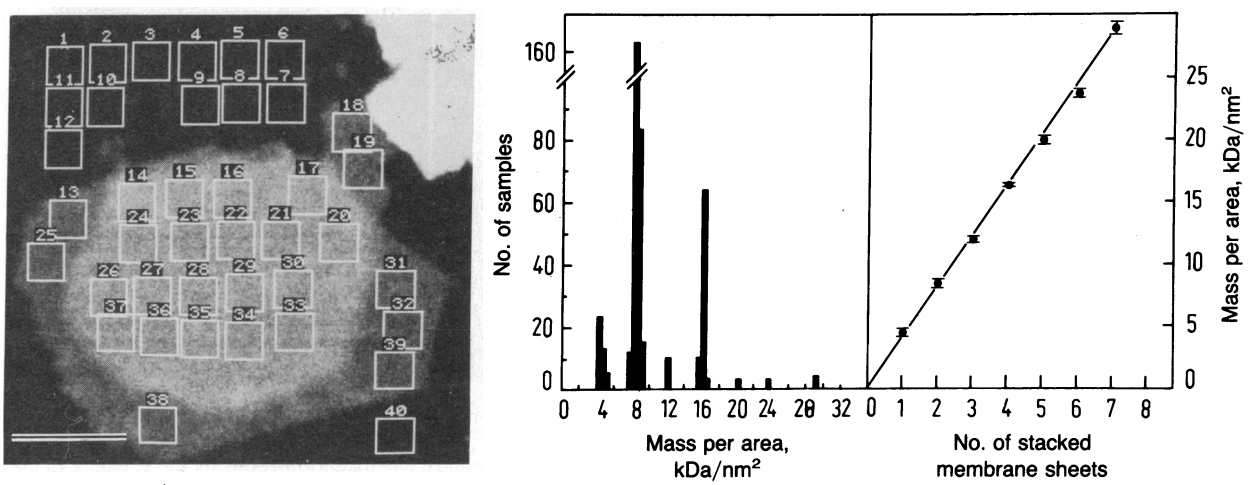

FIG. 2. STEM mass determination of freeze-dried membranes of *E. halochloris*. The sample boxes represent areas selected for density determination of the single or multiply layered membranes and the carbon film. (Scale bar = 100 nm.) The histogram shows a discrete distribution of the mass per unit area according to the number of membranes stacked upon each other. The mass of the carbon support was subtracted.

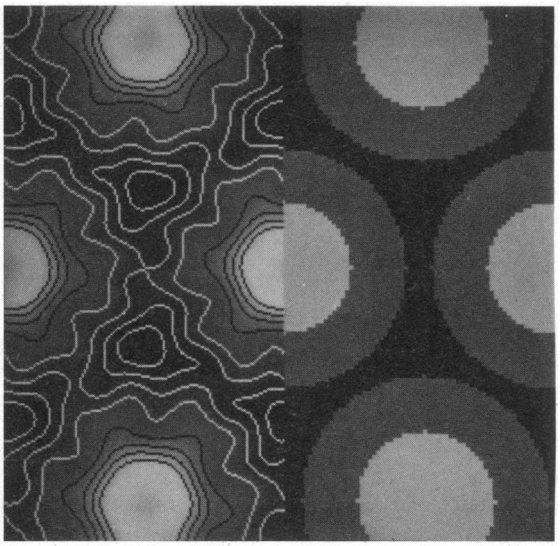

FIG. 3. Mass mapping of the photosynthetic unit: contoured average (*Left*) and mass map (*Right*). The densities of the three areas—i.e., the RC (bright), the ring of LH complexes (grey), and the remaining area, mainly containing lipids (black)—were integrated and corrected for the background level of the underlying carbon support.

tions to minimize radiation damage (6). Single layered membranes as well as stacked sheets were included in mass measurements (Fig. 2). The average mass per unit area (3.98 kDa/nm^2), derived from the slope of the regression line in Fig. 2, corresponds to a total mass of 573 ± 40 kDa for the unit cell (144 nm^2). While global mass determination is resolution independent, mass mapping involves averaging of extremely noisy images and, hence, depends on the resolution achieved (approximately 4 nm). Three major domains of the morphological unit can be distinguished: a central core, a ring containing six elongated complexes, and areas around the threefold symmetry axes representing the lipid bilayer (Fig. 3). The masses of the three domains (Table 2) yield a stoichiometric model of the photosynthetic unit. The mass of the central core is consistent with a 1:1:1:1(:1) ratio of the subunits cytochrome, H, M, L, (and "X"), including chromophores. The molecular masses of RC polypeptides tend either to be underestimated (L, M) or overestimated (H) in PAGE (20, 21). However, the apparent molecular mass of

Table 2. Mass estimates of substructures in the photosynthetic complex

Substructure	Mass determined by STEM, kDa	Stoichiometry	Calculated molecular mass,* kDa
RC + cytochrome	150 ± 10	$L_1M_1H_1Cyt_1$	140 ± 7
LH ring	272 ± 20	$6 \times (\alpha_2\beta_2\gamma_2)$	234 ± 20
Lipid bilayer	151 ± 10		

*Masses of the substructures were calculated by using the apparent molecular masses from PAGE and the stoichiometry assumed. Masses of the chromophores in the RC, 9 kDa; in one LH complex, 4 kDa (18, 19).

the RC (approximately 90 kDa without the bound cytochrome) corresponds to the value deduced from the sequence data of the *R. capsulata* RC (94.5 kDa) (20). If "X" is a component of the photosynthetic unit, it may be located close to the RC, since PAGE suggests that "X" occurs in approximately equimolar amounts with respect to the RC polypeptides.

The *p6* symmetry of the LH ring can be used as an additional constraint for evaluating the stoichiometry of the LH polypeptides. The mass of one LH complex, possibly containing some bound lipid, was estimated to be 45.6 ± 3.4 kDa. Assuming an equimolar ratio of the three components α, β, and γ (as outlined above), we obtain a stoichiometric composition of 2:2:2 (Table 2). The images of relief reconstructions and averages of negatively stained membranes show 12 subunits in the LH ring (Fig. 4). However, adjacent LH subunits appear not equivalent, providing some evidence that the morphological subunits differ from the smallest stoichiometric unit ($\alpha_1\beta_1\gamma_1$).

While the structure of the LH ring reflects the hexagonal arrangement of the photosynthetic complexes in the membrane, the RC cannot be expected to obey this crystallographic order. The analysis of freeze-dried and shadowed membranes revealed that the protrusion on the periplasmic membrane face—i.e., the cytochrome (22)—deviates from *p6* symmetry (5). The RC is not centrosymmetric and it may assume various orientations within the photosynthetic complexes, creating the impression of a strongly distorted lattice (Fig. 5). Selective averaging of shadowed complexes classified by using correspondence analysis shows the cytochrome in quite different positions (Fig. 5*C*). This may reflect either rotational motion of the RC as the studies of Mar *et al.* (23)

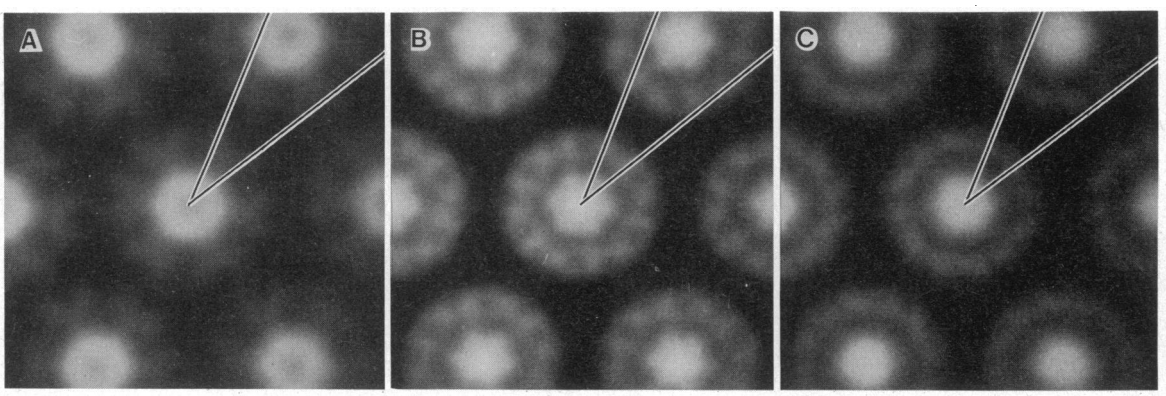

FIG. 4. Images of photosynthetic complexes from different preparations obtained after image processing (with the RC artificially symmetrized). (*A*) Average of an unstained membrane recorded in the STEM (elastic dark-field image); bright features represent high mass (protein). (*B*) Average of a negatively stained membrane obtained after selection of the most significant positions by the least-strain criterion. Heavily stained regions are black. (*C*) Surface relief reconstruction of the cytoplasmic face of freeze-dried and unidirectionally shadowed membranes. Bright areas represent features protruding from the lipid bilayer, dark areas indicate valleys. The resolutions achieved are 4, 2, and 1.8 nm, respectively. The subunits in the LH rings are oriented identically in all images with respect to the symmetry axis; the lines connecting the centers of the complexes and adjacent LH subunits elucidate the handedness in the LH ring. Lattice spacing is 13 nm.

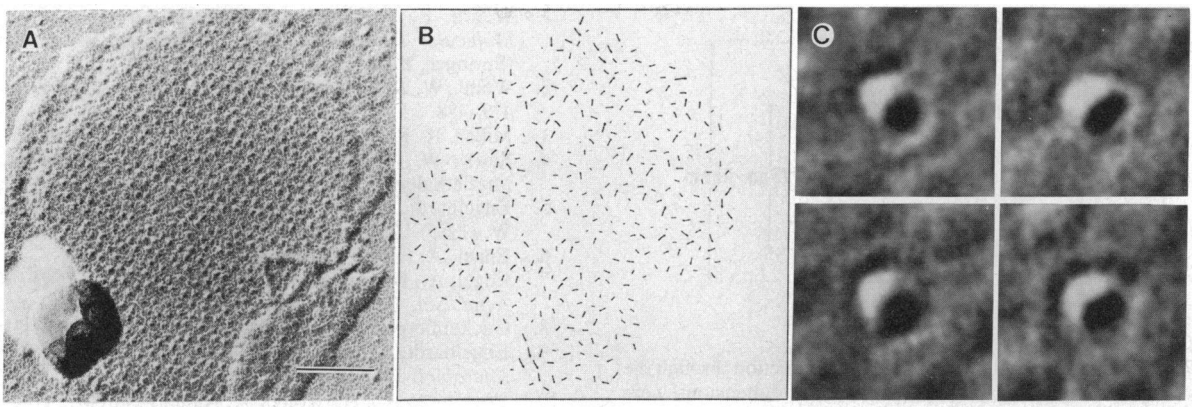

FIG. 5. (*A*) Image of the periplasmic surface of a unidirectionally shadowed membrane (tantalum/tungsten). The protrusions—i.e., the cytochromes—assume various orientations on the photosynthetic complexes, creating the impression of substantial lattice disorder. (Scale bar = 200 nm.) (*B*) The displacement vectors indicate the positions of the protrusions found and the displacements with respect to the nearest point of an ideal—i.e., least-squares-fitted—lattice. The vectors are magnified by a factor of 2. (*C*) Selective averages of photosynthetic complexes classified by means of correspondence analysis. The first two eigenvalues, related to the most significant differences among the complexes analyzed, were used for classification. The original image was low-pass filtered to a resolution of 2 nm prior to the extraction of 390 unit cells (for details see ref. 5). The image size is 22.5 nm.

suggest, or, if the RC were strongly fixed in position, the existence of various but equivalent orientations according to the internal symmetry of the LH ring. Rotational diffusion would enable the RC to assume equivalent positions relative to all LH complexes of the photosynthetic unit; this may have implications for the energy transfer. Careful inspection of images of shadowed *R. viridis* membranes shown in refs. 1, 4, 24, and 25 indicates that here also the cytochromes are variously oriented. There is strong evidence now from x-ray structure analysis that the asymmetric shape of the protrusion is a genuine feature; the cytochrome is clearly attached obliquely to the L and M subunits (18).

As a consequence of the variability among the (neighboring) photosynthetic units a three-dimensional reconstruction from a tilt series will clearly suffer from overlapping and averaging of nonequivalent unit cells. A prerequisite for a rigorous three-dimensional reconstruction would be to persuade all components of the photosynthetic units to assume equivalent positions. This might be accomplished by illumination with polarized light. Data on the three-dimensional structure of the photosynthetic complex have been obtained here by relief reconstruction (5, 8) of unidirectionally shadowed membranes. This method in conjunction with selective averaging has proved to be useful, since it is capable of taking into account the inherent deviations from crystallinity and allows the surfaces to be reconstructed separately. In Fig. 6, views of the two surfaces are presented, and Fig. 7 schematically summarizes the transmembrane structure of the photosynthetic unit. According to ref. 18, the central mass on the cytoplasmic face should represent the H subunit. The part of the RC located in the membrane interior is estimated to have a mass of approximately 150 kDa, if a cylindrical shape with a diameter of 7 nm (as deduced from the mass map) is assumed. The calculated mass is substantially greater than the 60–80 kDa expected (L and M subunits and some additional mass from the other RC polypeptides). Rather, these data suggest that the RC has an elliptical projection area with diameters of 7 nm and 2.8–3.7 nm. This corresponds to the x-ray structure analysis of the *R. viridis* RC (18).

The structural similarity between the photosynthetic membranes of *E. halochloris* and *R. viridis* is striking (9). In fact, the two-dimensional maps presented by Stark *et al.* (4) are quite similar to our reconstructions with the exception that the apparent positional variability of the cytochrome is disguised by averaging and forcing sixfold symmetry. The three-dimensional model of the negatively stained photosynthetic unit from *R. viridis*, published by Miller (3), suggests that the LH ring consists of six compact complexes oriented towards the threefold symmetry axes, which is in contrast to our results. The number of morphological subunits of this model might be related to limited lateral resolution. However, the presence of globular masses within the lipid bilayer

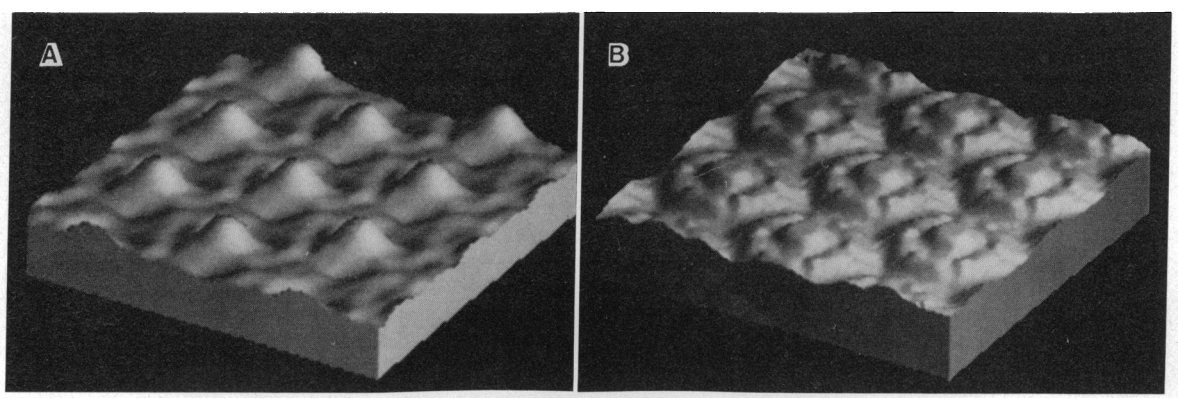

FIG. 6. Three-dimensional representation of the surface reliefs of the photosynthetic membrane obtained from freeze-dried and unidirectionally shadowed preparations. The periplasmic surface (*A*) was reconstructed from a selective average obtained by correspondence analysis (Fig. 5*C*). The ring of LH complexes is created partly due to the noncentrosymmetric position of the cytochrome; symmetry was not enforced. With the cytoplasmic face (*B*) sixfold symmetry was assumed and enforced. The reliefs are scaled in the *z* direction; the borders indicate the lipid bilayer (5 nm thick).

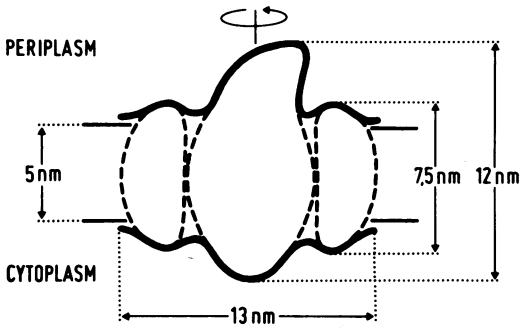

FIG. 7. Schematic model of a transmembrane section through the photosynthetic complex. Data on the shape and dimensions were drawn from surface relief reconstructions and averages of negatively stained and unstained membranes. The rotation symbol indicates that the RC may assume various orientations in the LH rings. The cytochrome protrudes approximately 4 nm, and the opposite part of the RC, 2.8 nm beyond the surface of the lipid bilayer. The maximum heights of the LH complexes are about 1 and 1.5 nm, respectively.

region, which is not accessible to negative stain and, hence, is invisible, must probably be attributed to artifacts created by reconstruction (elongation of the point response in the z direction due to the "missing cone") and inappropriate thresholding (in the course of model building).

An interesting aspect of our results is that the polypeptide pattern, the mass determination, and the pattern of substructures in the various averages consistently show no indication of the presence of protein complexes in addition to the photosynthetic units. Thus, other components of energy conservation, such as the ATPase, must be assumed to be outside the regular arrays, implying the necessity of, for example, lateral translocation of protons.

We thank Dr. J. Peters for valuable advice with cross-linking experiments and Mrs. U. Santarius and Mr. J. Lubiniecki for skillful technical assistance. Parts of this work were supported by grants from the European Molecular Biology Organization and the Swiss National Foundation for Scientific Research.

1. Wehrli, E. & Kübler, O. (1980) in *Electron Microscopy at Molecular Dimensions*, eds. Baumeister, W. & Vogell, W. (Springer, Berlin), pp. 48–56.
2. Welte, W. & Kreutz, W. (1982) *Biochim. Biophys. Acta* **692,** 479–488.
3. Miller, K. R. (1982) *Nature (London)* **300,** 53–55.
4. Stark, W., Kühlbrandt, W., Wildhaber, I., Wehrli, E. & Mühlethaler, K. (1984) *EMBO J.* **3,** 777–783.
5. Engelhardt, H., Guckenberger, R., Hegerl, R. & Baumeister, W. (1985) *Ultramicroscopy* **16,** 395–410.
6. Engel, A. (1978) *Ultramicroscopy* **3,** 273–281.
7. Engel, A., Baumeister, W. & Saxton, W. O. (1982) *Proc. Natl. Acad. Sci. USA* **79,** 4050–4054.
8. Guckenberger, R. (1985) *Ultramicroscopy* **16,** 357–370.
9. Engelhardt, H., Baumeister, W. & Saxton, W. O. (1983) *Arch. Microbiol.* **135,** 169–175.
10. Hashimoto, F., Horigome, T., Kanbayashi, M., Yoshida, K. & Sugano, H. (1983) *Anal. Biochem.* **129,** 192–199.
11. Thomas, P. E., Ryan, D. & Levin, W. (1976) *Anal. Biochem.* **75,** 168–176.
12. Saxton, W. O. & Baumeister, W. (1982) *J. Microsc. (Oxford)* **127,** 127–138.
13. Saxton, W. O. & Baumeister, W. (1982) *Inst. Phys. Conf. Ser.* **61,** 333–336.
14. Frank, J., Verschoor, A. & van Heel, M. (1982) *J. Mol. Biol.* **161,** 107–137.
15. Thornber, J. P., Cogdell, R. J., Seftor, R. E. B. & Webster, G. D. (1980) *Biochim. Biophys. Acta* **593,** 60–75.
16. Steiner, R. & Scheer, H. (1985) *Biochim. Biophys. Acta* **807,** 278–284.
17. Brunisholz, R. A., Jay, F., Suter, F. & Zuber, H. (1985) *Biol. Chem. Hoppe-Seyler* **366,** 87–98.
18. Deisenhofer, J., Epp, O., Miki, K., Huber, R. & Michel, H. (1984) *J. Mol. Biol.* **180,** 385–398.
19. Oelze, J. (1981) *Sub-Cell. Biochem.* **8,** 1–73.
20. Youvan, D. C., Bylina, E. J., Alberti, M., Begusch, H. & Hearst, J. E. (1984) *Cell* **37,** 949–957.
21. Michel, H., Weyer, H., Gruenberg, H. & Lottspeich, F. (1985) *EMBO J.* **4,** 1667–1672.
22. Then, J. & Trüper, H. G. (1984) *Arch. Microbiol.* **139,** 295–298.
23. Mar, T., Picorel, R. & Gingras, G. (1981) *Biochim. Biophys. Acta* **637,** 546–550.
24. Miller, K. R. (1979) *Proc. Natl. Acad. Sci. USA* **76,** 6415–6419.
25. Jay, F., Lambillotte, M. & Mühlethaler, K. (1983) *Eur. J. Cell Biol.* **30,** 1–8.